Preparation and adsorption properties of a facile solid cucurbit[8]uril-based porous supramolecular assembly

Chun Chun Chen,[†] Wei-Wei Ge,[‡] Kai Chen,*[,‡] Zhu Tao,*[,†] Yun Qian Zhang,[†] Qian Jiang Zhu[†]

[†]Key Laboratory of Macrocyclic and Supramolecular Chemistry of Guizhou Province, Guizhou University, Guiyang 550025, People's Republic of China.

[‡]Collaborative Innovation Center of Atmospheric Environment and Equipment Technology, Jiangsu Key Laboratory of Atmospheric Environment Monitoring and Pollution Control, School of Environmental Science and Engineering, Nanjing University of Information Science & Technology, Nanjing 210044, People's Republic of China.

EXPERIMENTAL SECTION

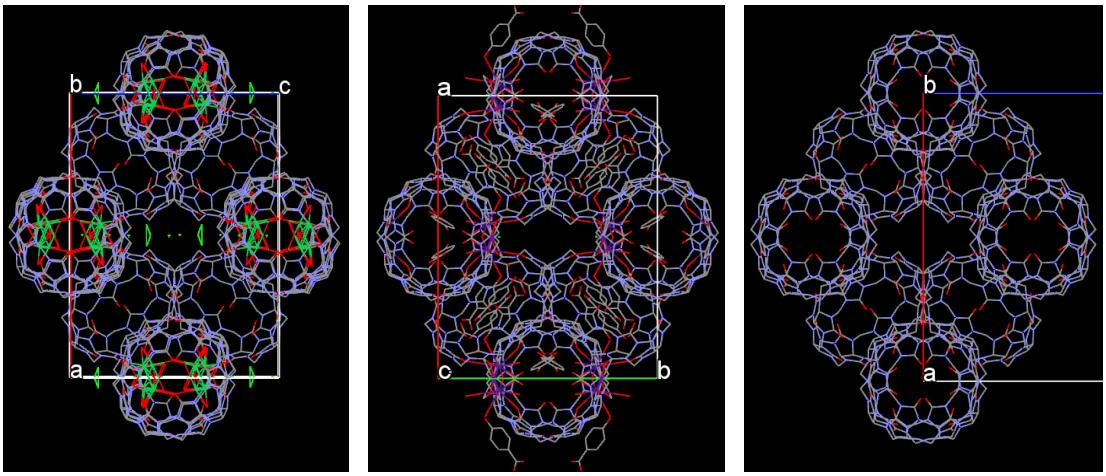

a b c

Fig. S1 Similar structure features from different Q[8]-based supramolecular assemblies by using different methods.

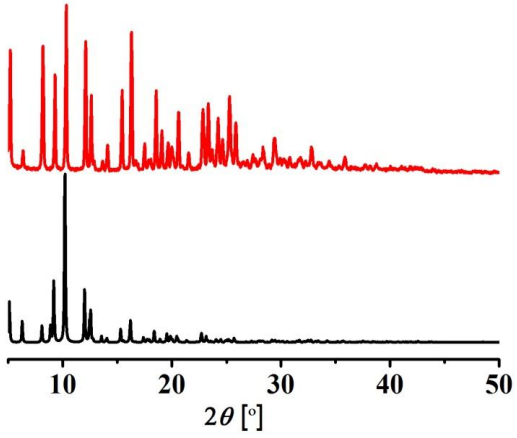

Fig. S2 Powder X-ray diffraction analyses of **A** (top) and comparison with simulation (bottom)

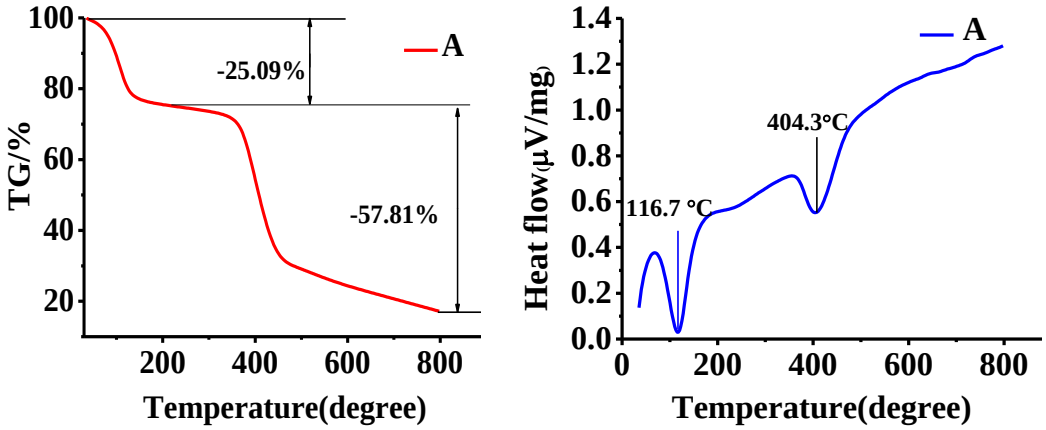

Fig. S3. TG (left) and DTA (right) curves of **A** in N_2.

Table S1 General survey of loading **A** with 17 fluorophore guests (**FG**s) to form luminescent materials (**FG@A**s); (first column) 17 **FG**s; (second column) comparison of colours under daylight and UV-light (365nm) and comparison of fluorescence spectra of **FG**s and solid **FG@A**s.

λ_{maxem} Colour	Survey of loading **A** with **G** (saturated adsorption)
434nm **Voilet** 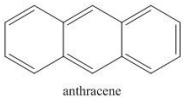 anthracene **FG1**	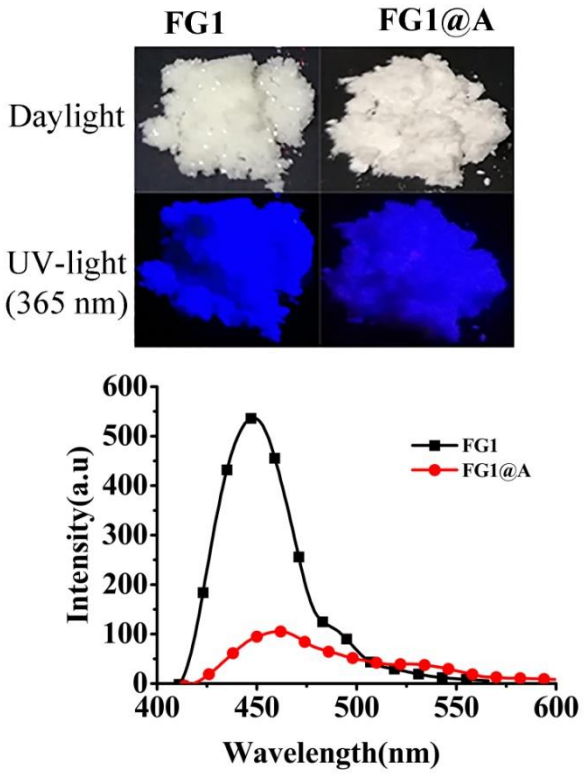

607nm **Red** 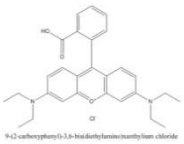 **FG**2	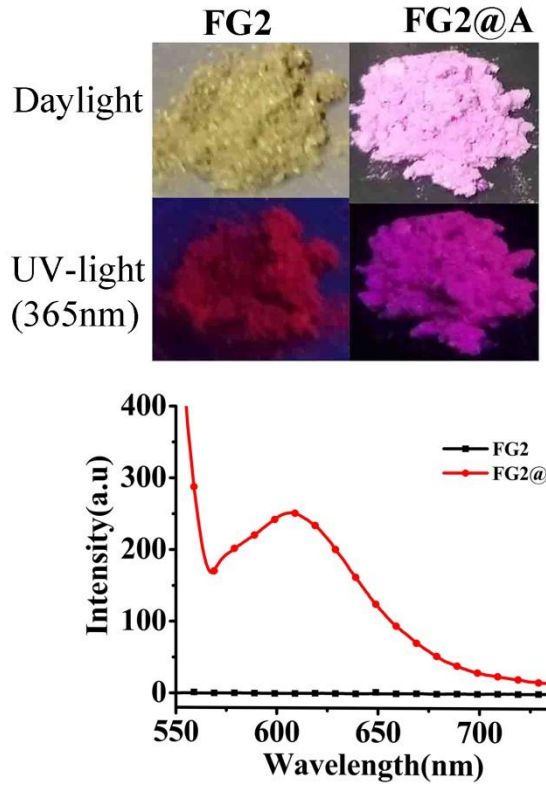
340nm **Voilet** 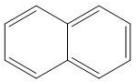 naphthalene **FG**3	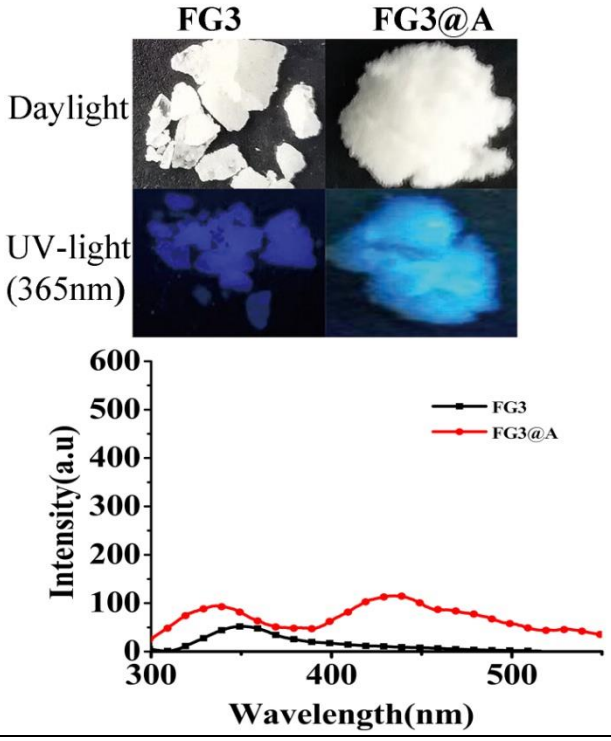

378nm **Voilet** 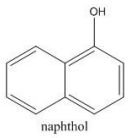 **FG**4	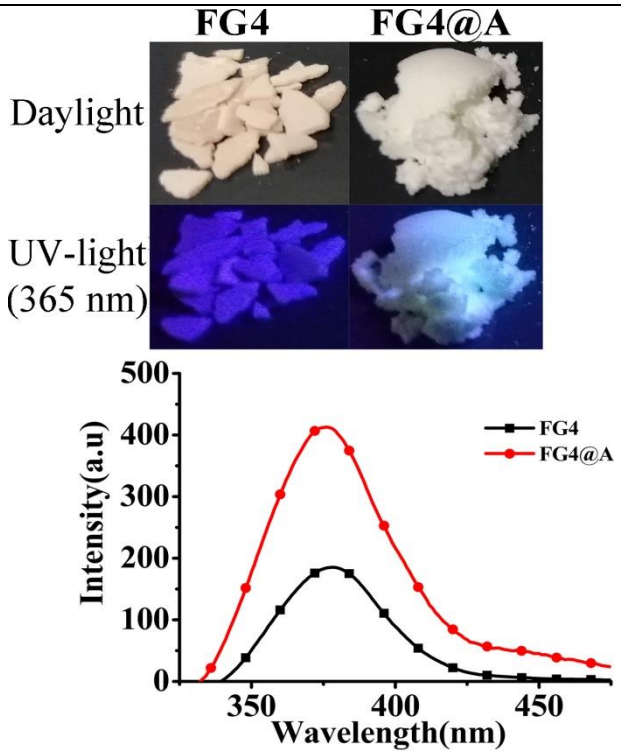
384nm Voilet 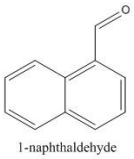 **FG**5	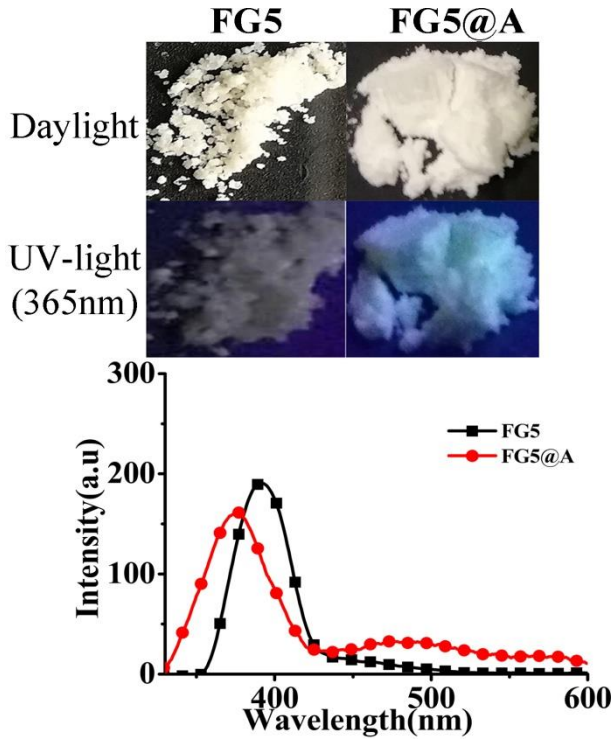

560nm **Green** 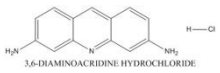 3,6-DIAMINOACRIDINE HYDROCHLORIDE **FG**6	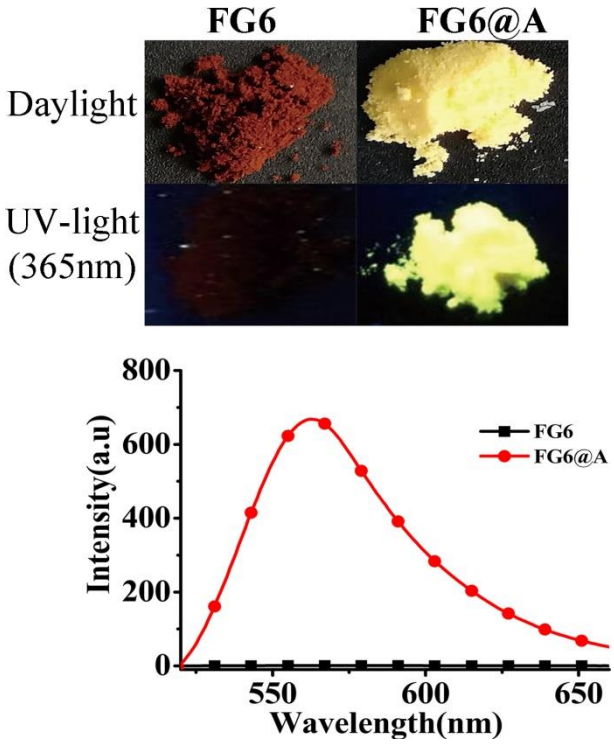
477nm Blue 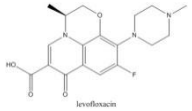 levofloxacin **FG**7	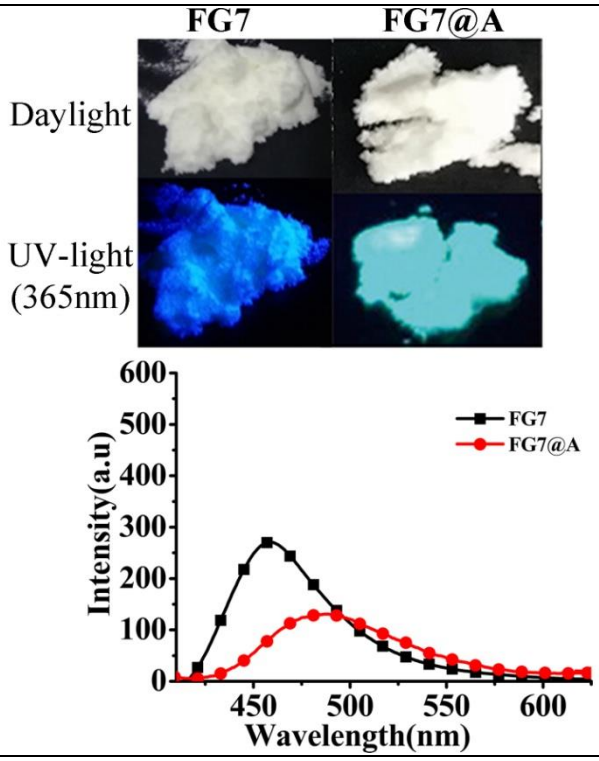

469nm → 392nm **blue→voilet** 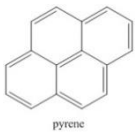 pyrene **FG8**	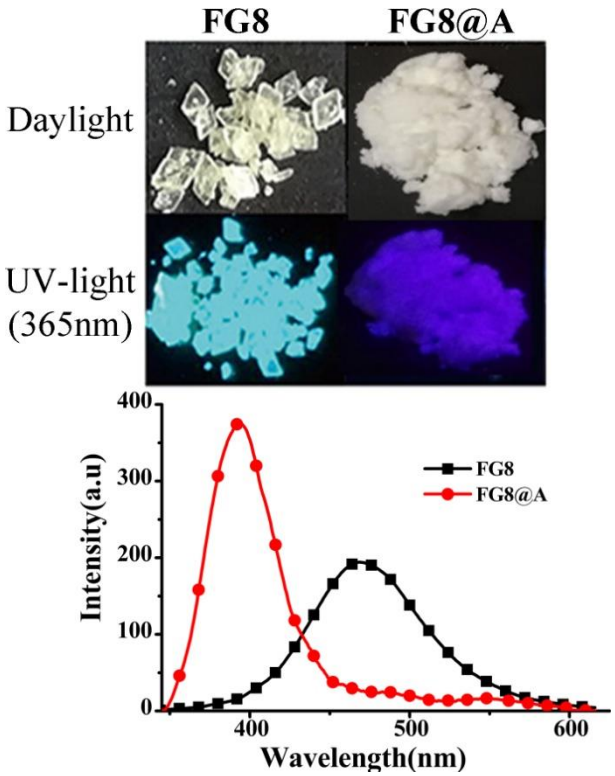
560nm **Green** 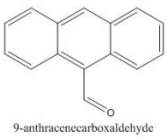 9-anthracenecarboxaldehyde **FG9**	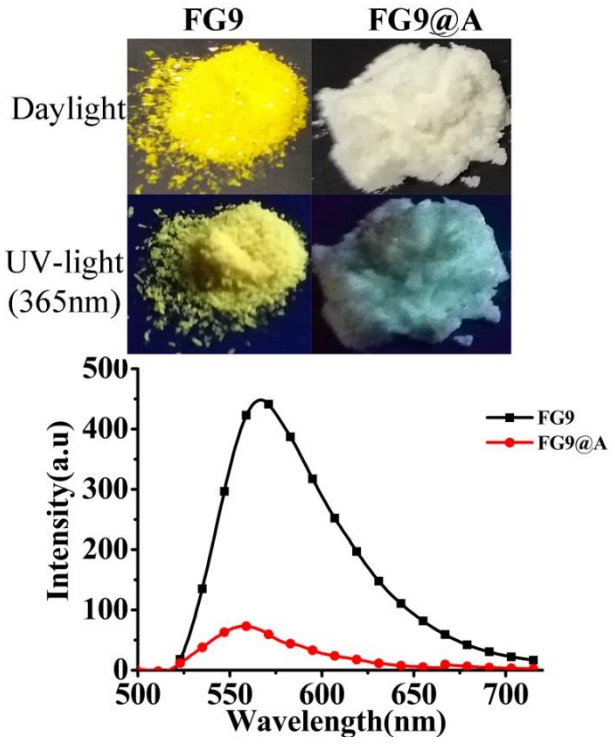

420nm **Violet** 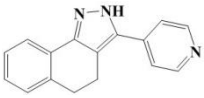 **FG**10	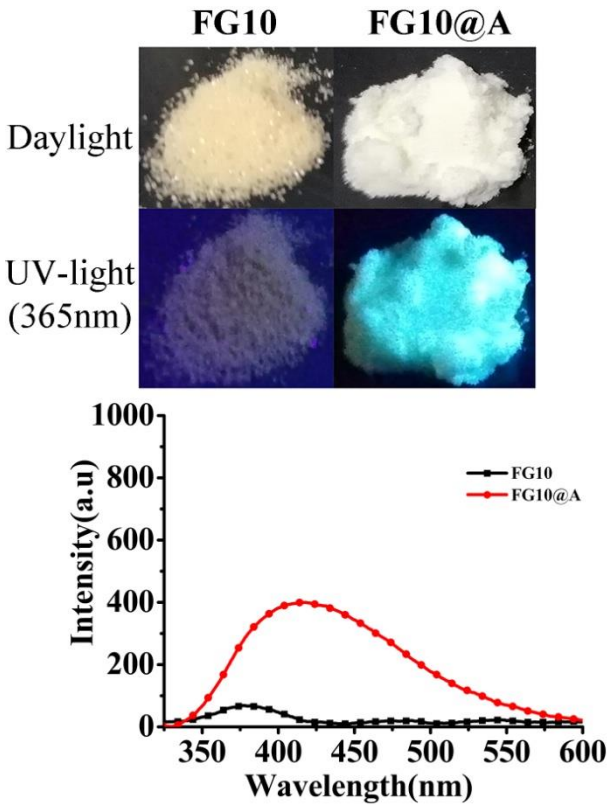
561nm Green 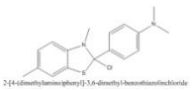 **FG**11	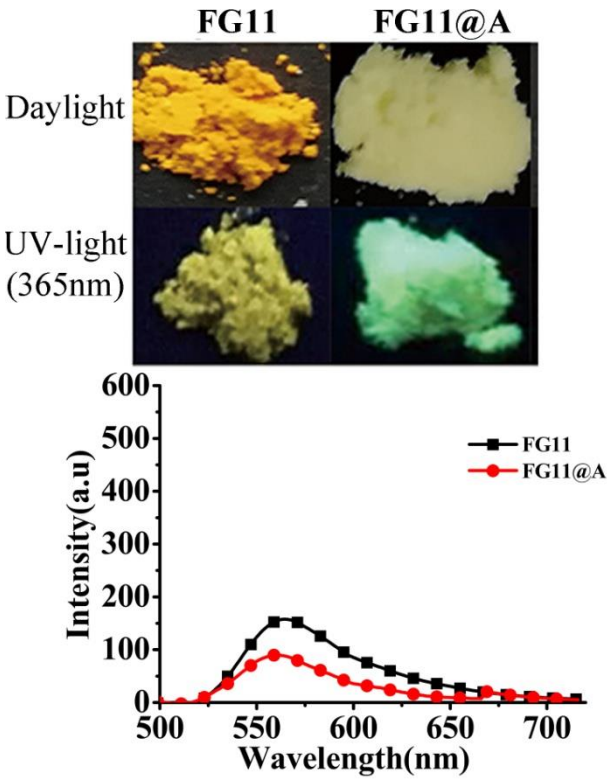

561nm Green 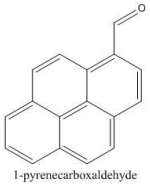 1-pyrenecarboxaldehyde **FG**12	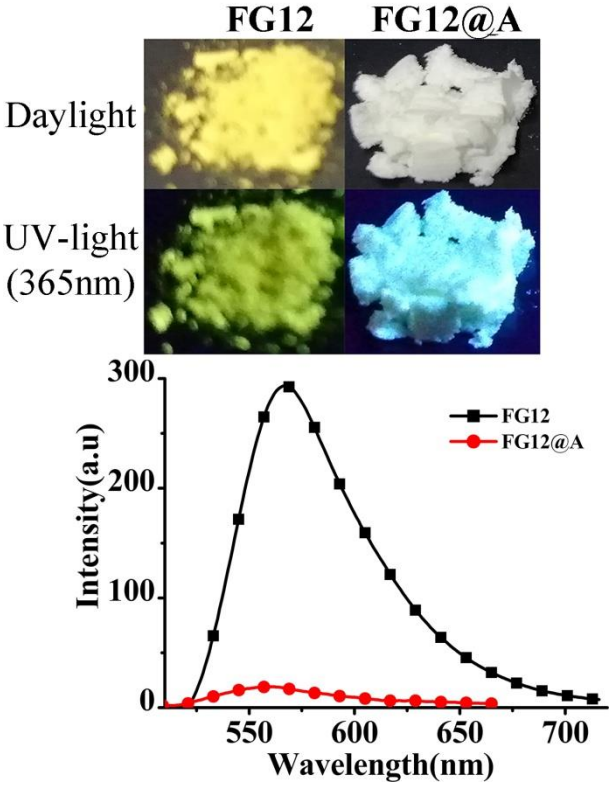
557 Green 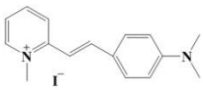 **FG**13	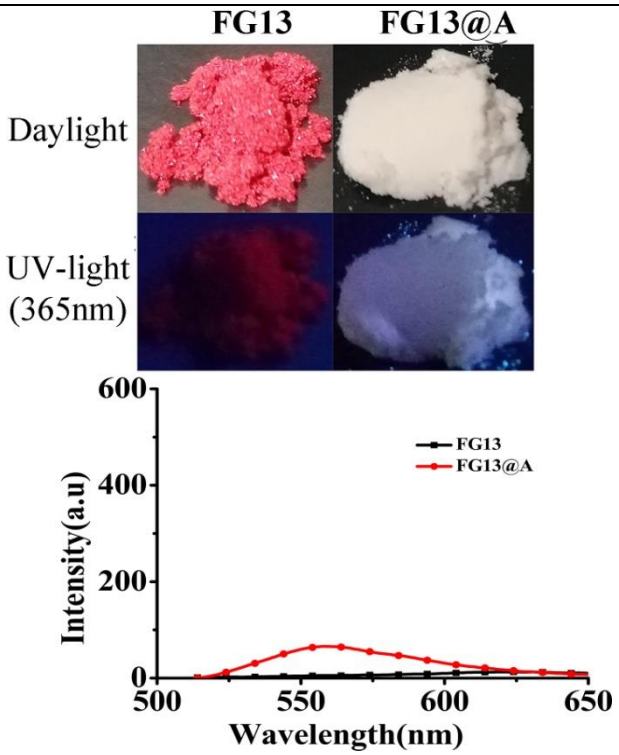

470nm Blue 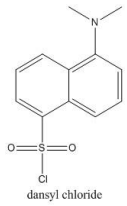 dansyl chloride **FG**14	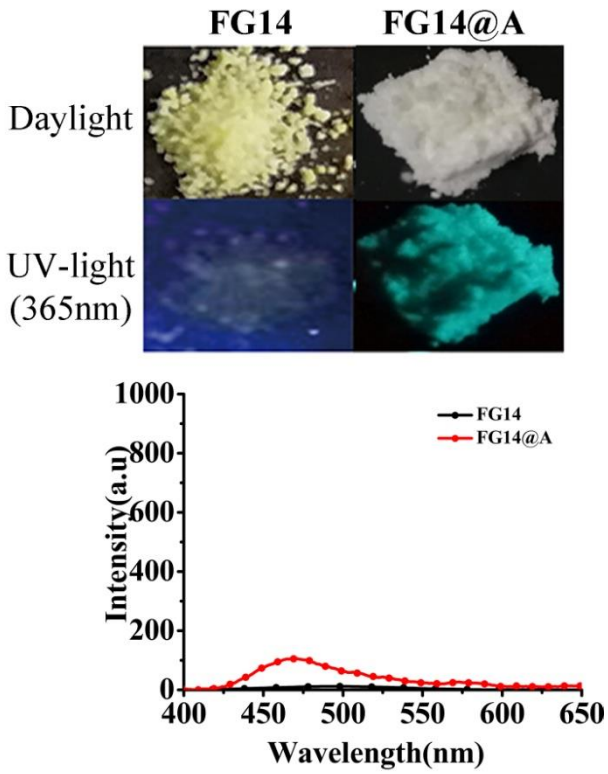
470nm Blue 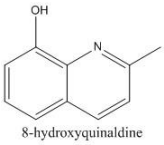 8-hydroxyquinaldine **FG**15	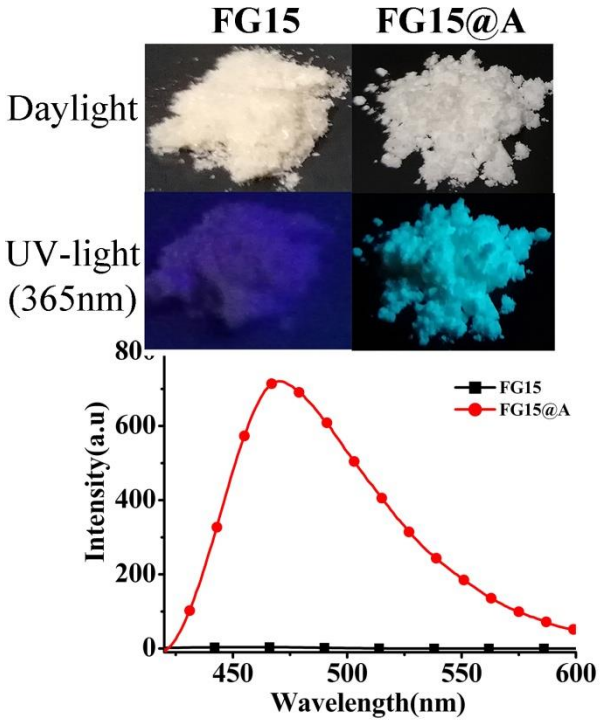

397nm/456nm **Voilet/blue** 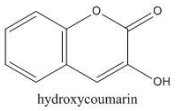 hydroxycoumarin **FG**16	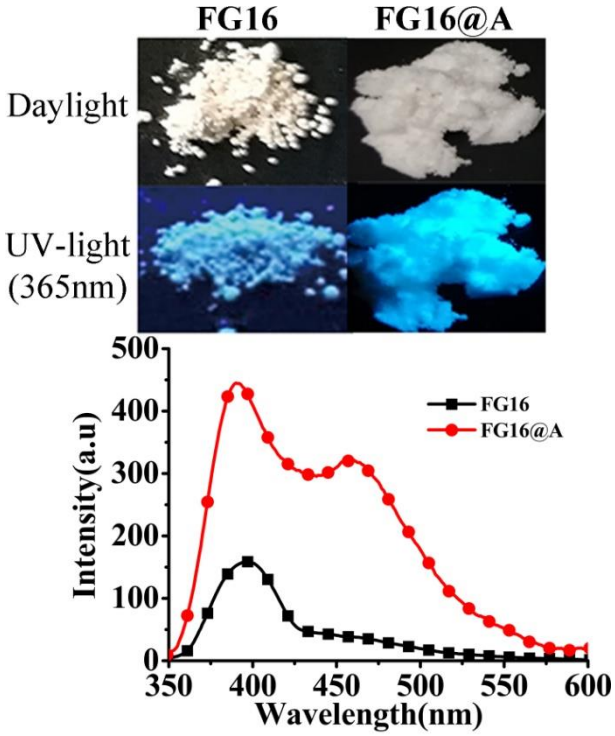
410nm/371nm 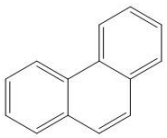 phenanthrene **FG**17	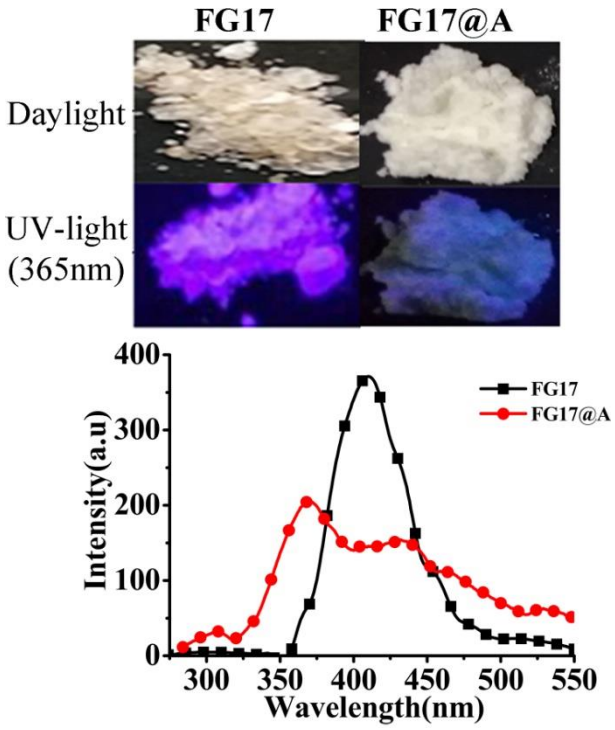

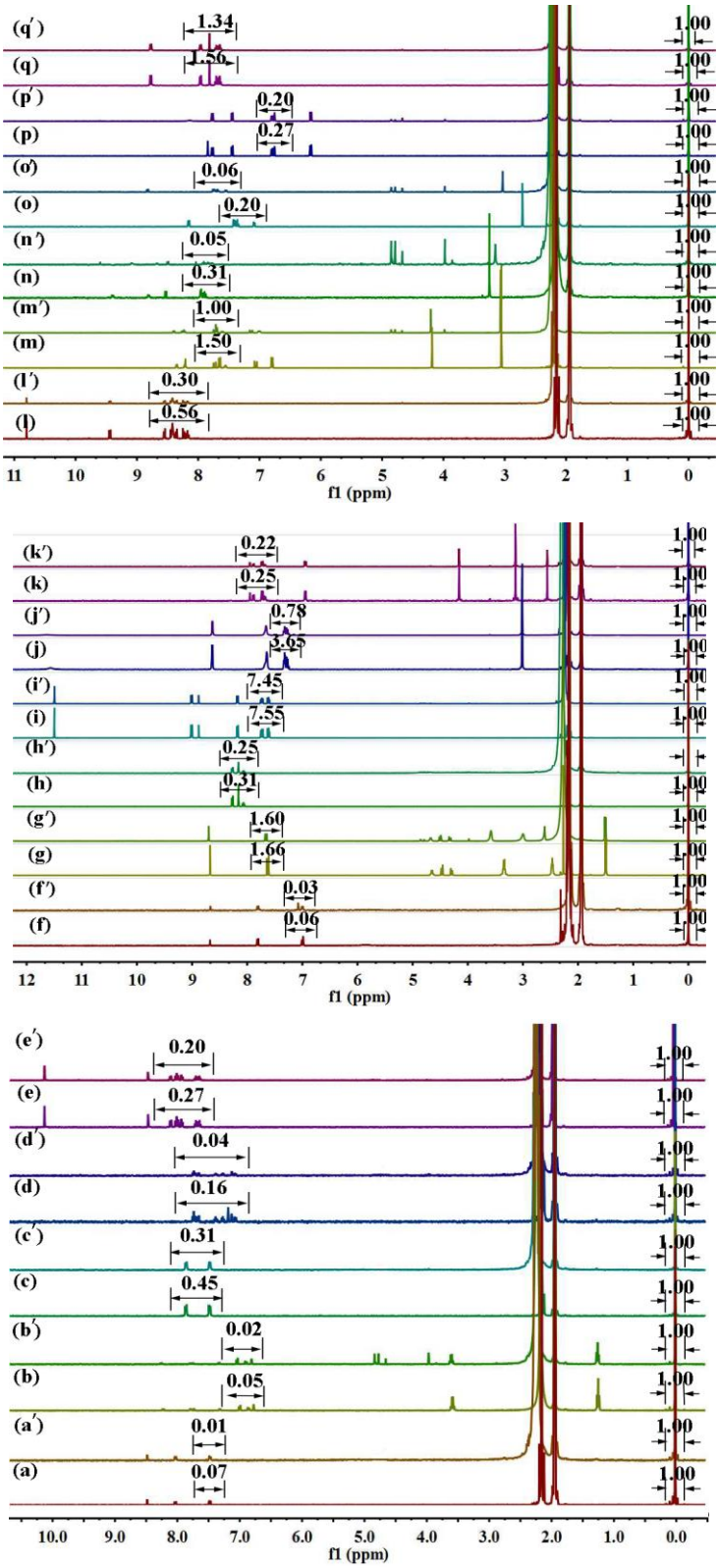

Fig. S4. ^{1}H NMR spectra in deuterated acetonitrile 0.5 mL 0.01 M **FG**x added 10 mg **A**: (a and a') **FG**1; (b and b') **FG**2; (c and c') **FG**3; (d and d') **FG**4; (e and e') **FG**5; (f and f') **FG**6; (g and g') **FG**7; (h and h') **FG**8; (i and i') **FG**9; (j and j') **FG**10; (k and k') **FG**11; (l and l') **FG**12; (m and m') **FG**13; (n and n') **FG**14; (o and o') **FG**15; (p and p') **FG**16; (q and q') **FG**17 before and after being adsorbed, respectively.

Table S2 Normalized adsorption capacities of Q[8]-based supramolecular assemblies (**A**) for the 17 selected **FG**s (mol/g)

FGs	A	FGs	A
(a') FG1@A	4.28×10^{-5}	**(j') FG10@A**	3.93×10^{-5}
(b') FG2@A	3.00×10^{-5}	**(k') FG11@A**	6.00×10^{-5}
(c') FG3@A	1.55×10^{-5}	**(l') FG12@A**	2.32×10^{-5}
(d') FG4@A	3.75×10^{-5}	**(m') FG13@A**	1.67×10^{-5}
(e') FG5@A	1.29×10^{-5}	**(n') FG14@A**	4.19×10^{-5}
(f') FG6@A	2.50×10^{-5}	**(o') FG15@A**	3.50×10^{-5}
(g') FG7@A	1.80×10^{-6}	**(p') FG16@A**	1.29×10^{-5}
(h') FG8@A	9.67×10^{-6}	**(q') FG17@A**	7.05×10^{-6}
(i') FG9@A	6.62×10^{-7}		

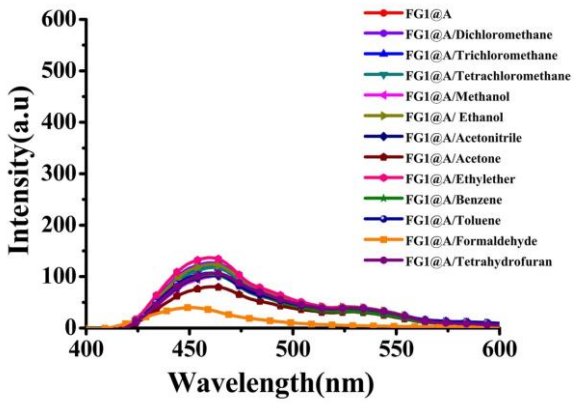

Fig. S5. General survey of fluorescence spectra of **FG**1@**A** loaded with the 12 respective **VOC**s.

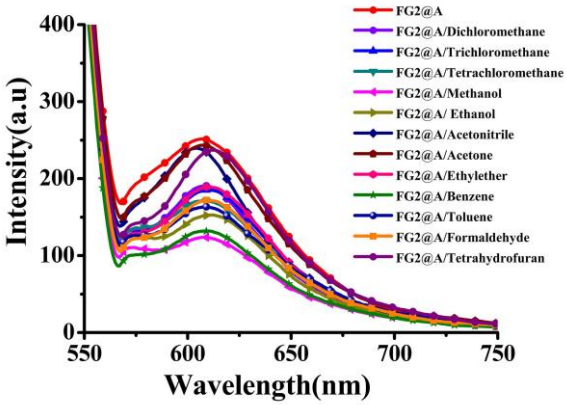

Fig. S6. General survey of fluorescence spectra of **FG**2@**A** loaded with the 12 respective **VOC**s.

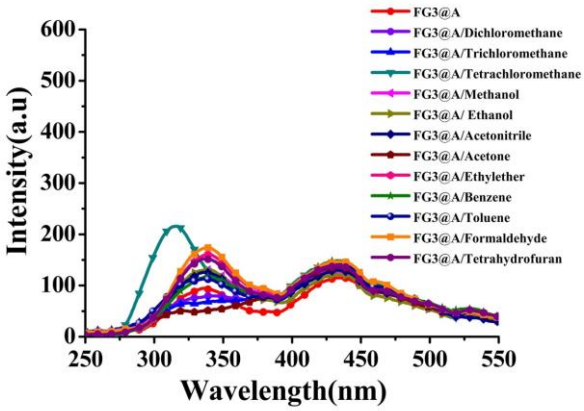

Fig. S7. General survey of fluorescence spectra of **FG**3@**A** loaded with the 12 respective **VOC**s.

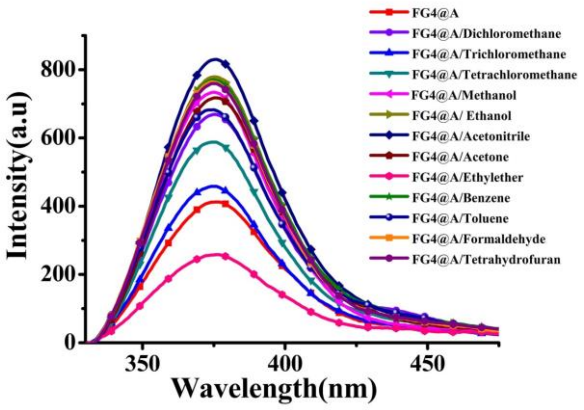

Fig. S8. General survey of fluorescence spectra of **FG**4@**A** loaded with the 12 respective **VOC**s.

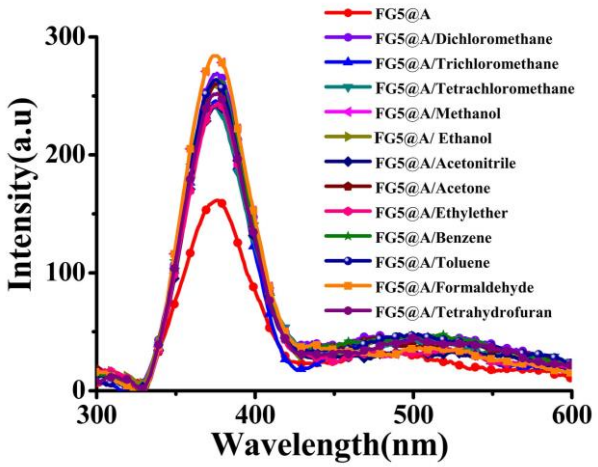

Fig. S9. General survey of fluorescence spectra of **FG**5@**A** loaded with the 12 respective **VOC**s.

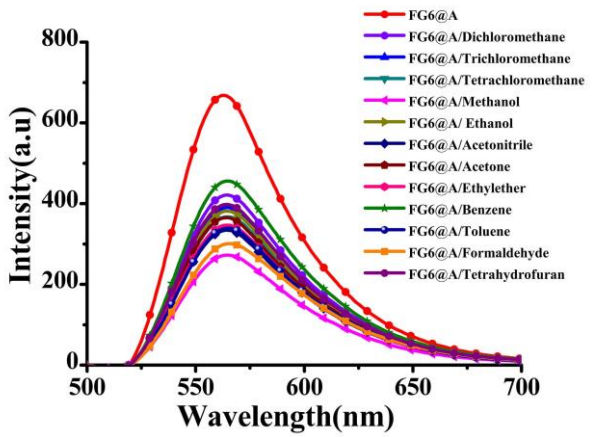

Fig. S10. General survey of fluorescence spectra of **FG**6@**A** loaded with the 12 respective **VOC**s.

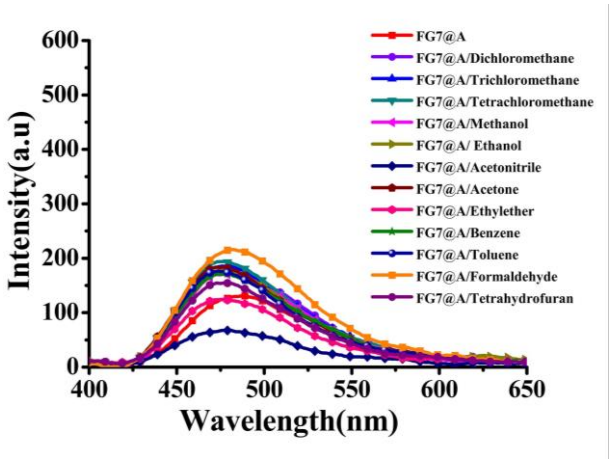

Fig. S11. General survey of fluorescence spectra of **FG**7@**A** loaded with the 12 respective **VOC**s.

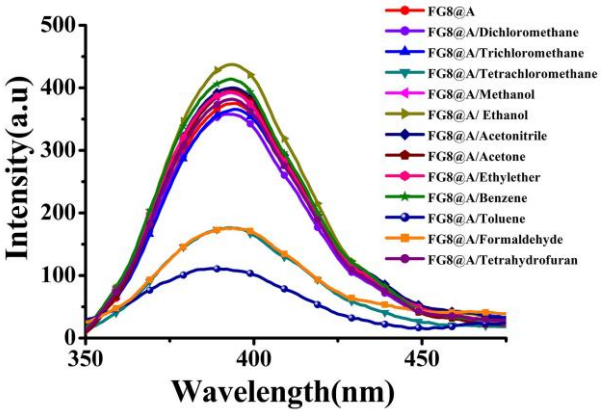

Fig. S12. General survey of fluorescence spectra of **FG**8@**A** loaded with the 12 respective **VOC**s.

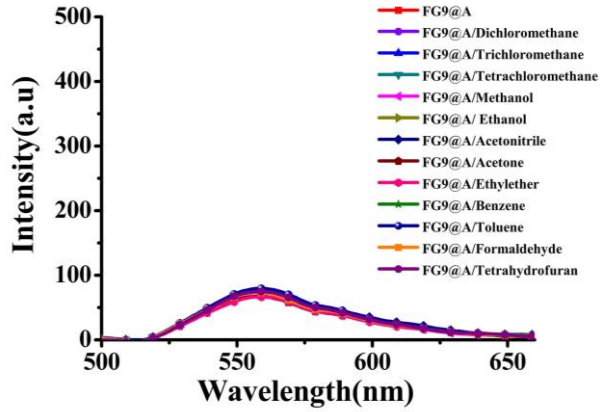

Fig. S13. General survey of fluorescence spectra of **FG**9@**A** loaded with the 12 respective **VOC**s.

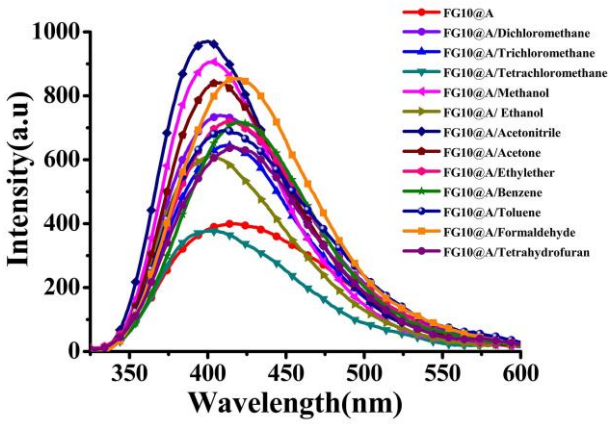

Fig. S14. General survey of fluorescence spectra of **FG**10@**A** loaded with the 12 respective **VOC**s.

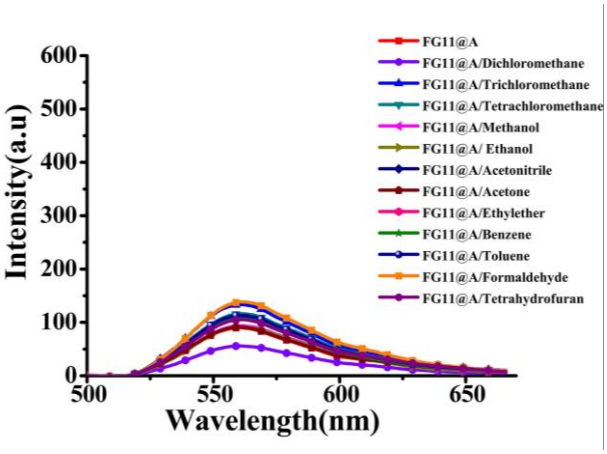

Fig. S15. General survey of fluorescence spectra of **FG**11@**A** loaded with the 12 respective **VOC**s.

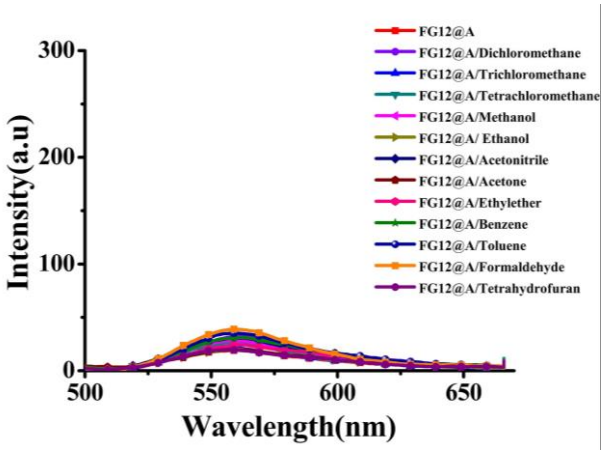

Fig. S16. General survey of fluorescence spectra of **FG**12@**A** loaded with the 12 respective **VOC**s.

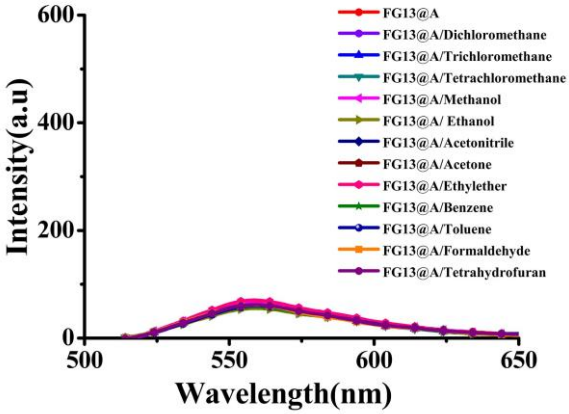

Fig.S17. General survey of fluorescence spectra of **FG**13@**A** loaded with the 12 respective **VOC**s.

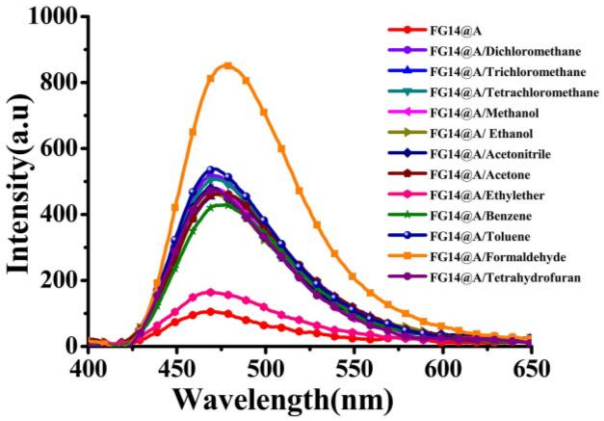

Fig. S18. General survey of fluorescence spectra of **FG**14@**A** loaded with the 12 respective **VOC**s.

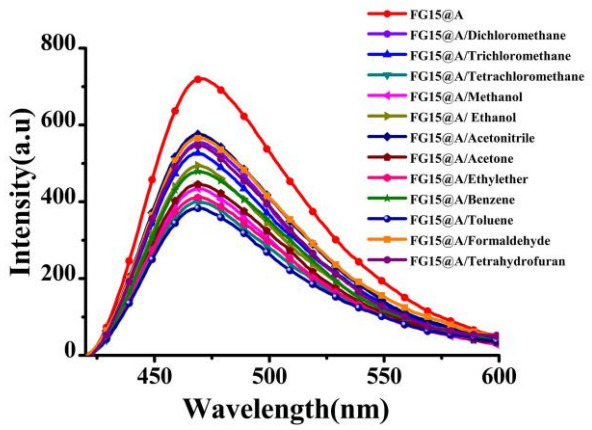

Fig. S19. General survey of fluorescence spectra of **FG**15@**A** loaded with the 12 respective **VOC**s.

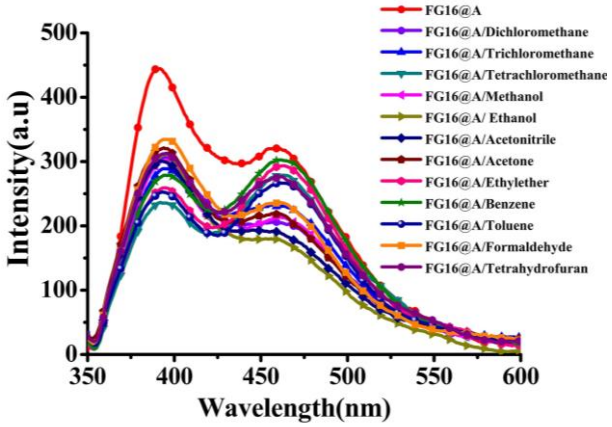

Fig. S20. General survey of fluorescence spectra of **FG**16@**A** loaded with the 12 respective **VOC**s.

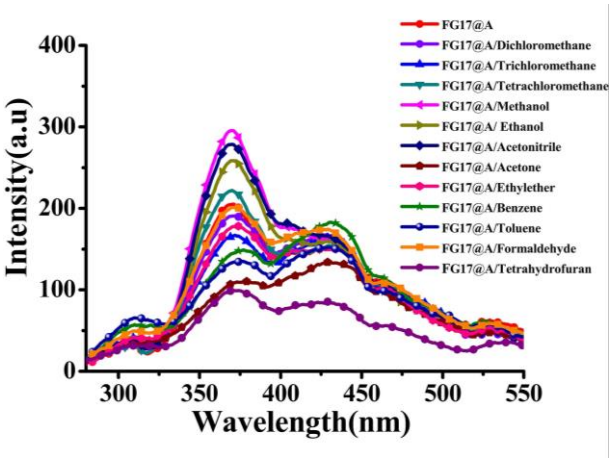

Fig. S21. General survey of fluorescence spectra of **FG**17@**A** loaded with the 12 respective **VOC**s.

The detection limits computational formula is $DL=C_{FG} \times 3 \times 0.05 \times C_{VOC} / k$

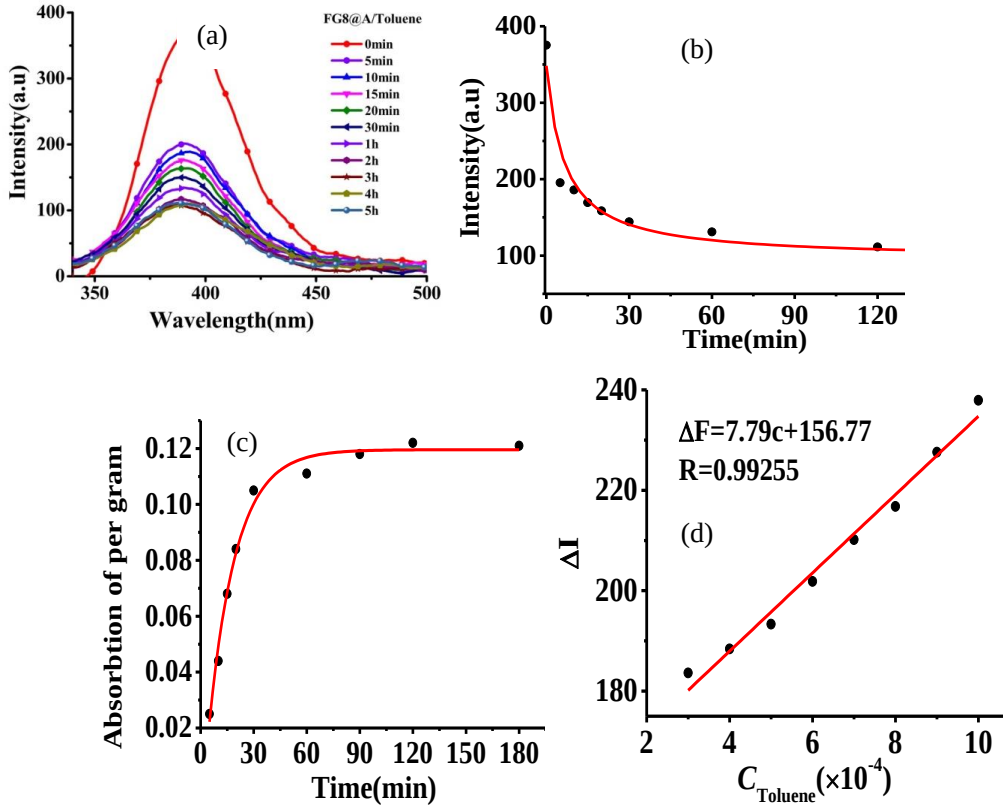

Fig. S22. (a) Titration fluorescence spectra of the loading of **FG**8@**A** with toluene; (b) change in fluorescence intensity of **FG**8@**A** with increasing adsorption time; (c) adsorption profile of the loading of toluene in **FG**8@**A**; (d) plot of ΔI *vs*. the amount of toluene adsorbed by solid **FG**8@**A**.

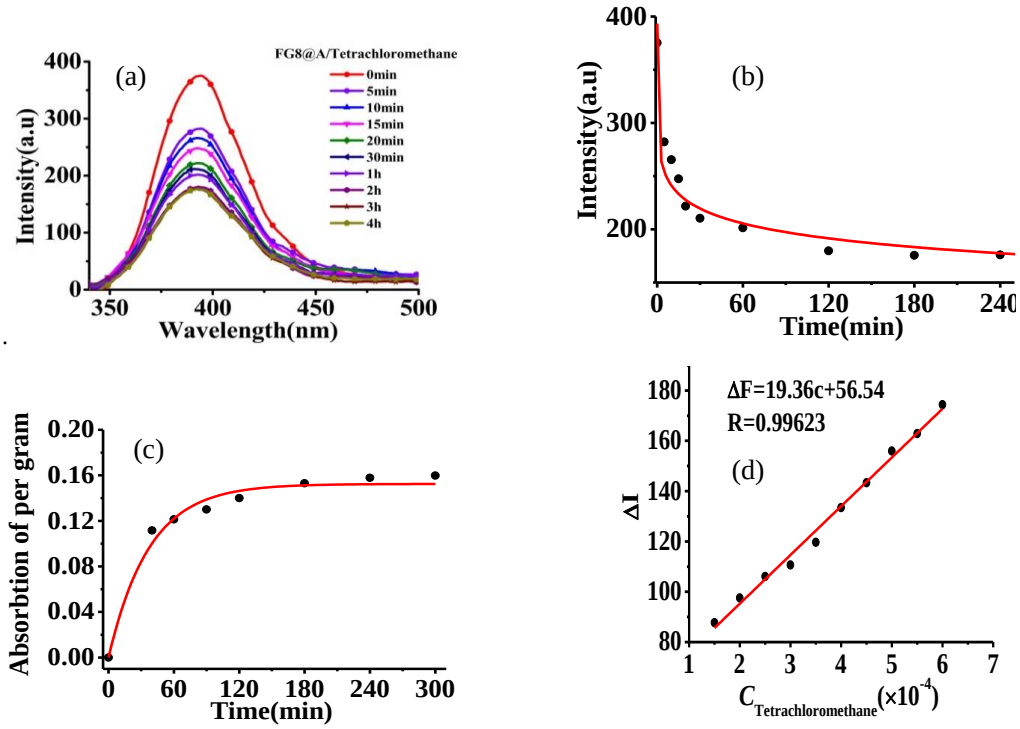

Fig. S23. (a) Titration fluorescence spectra of the loading of **FG**8@**A** with tetrachloromethane; (b) change in fluorescence intensity of **FG**8@**A** with increasing adsorption time; (c) adsorption profile of the loading of tetrachloromethane in **FG**8@**A**; (d) plot of ΔI *vs*. the amount of tetrachloromethane adsorbed by solid **FG**8@**A**.

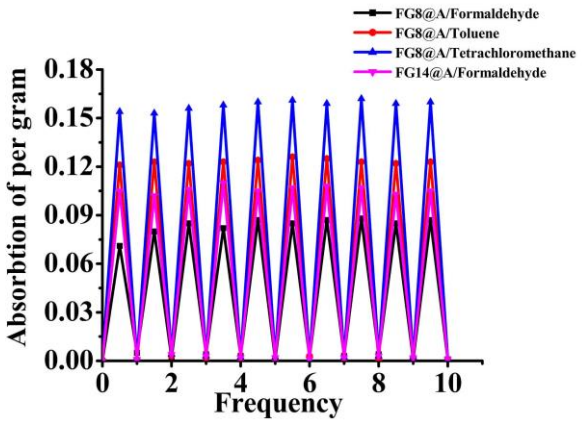

Fig. S24. Lifetime experiments of adsorption capacities of two selected solid **FG**8@**A** and **FG**14@**A** for selected volatile compounds.

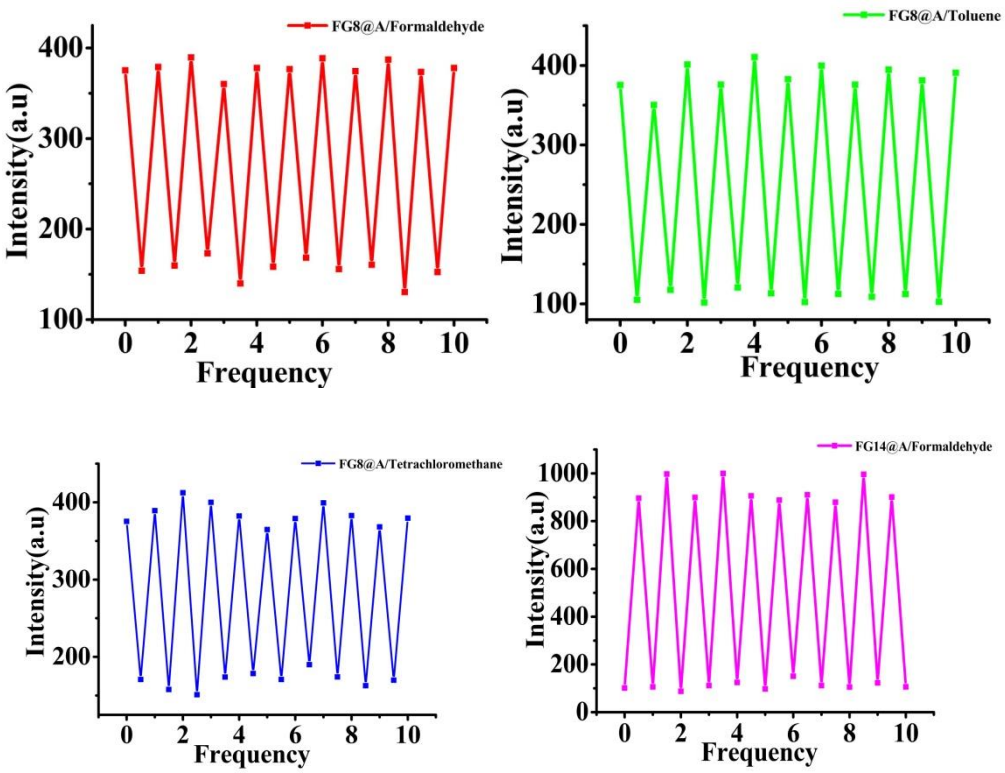

Fig. S25. Lifetime experiments of fluorescence strength of solid **FG**8@**A** and **FG**14@**A** for the selected volatile compounds.

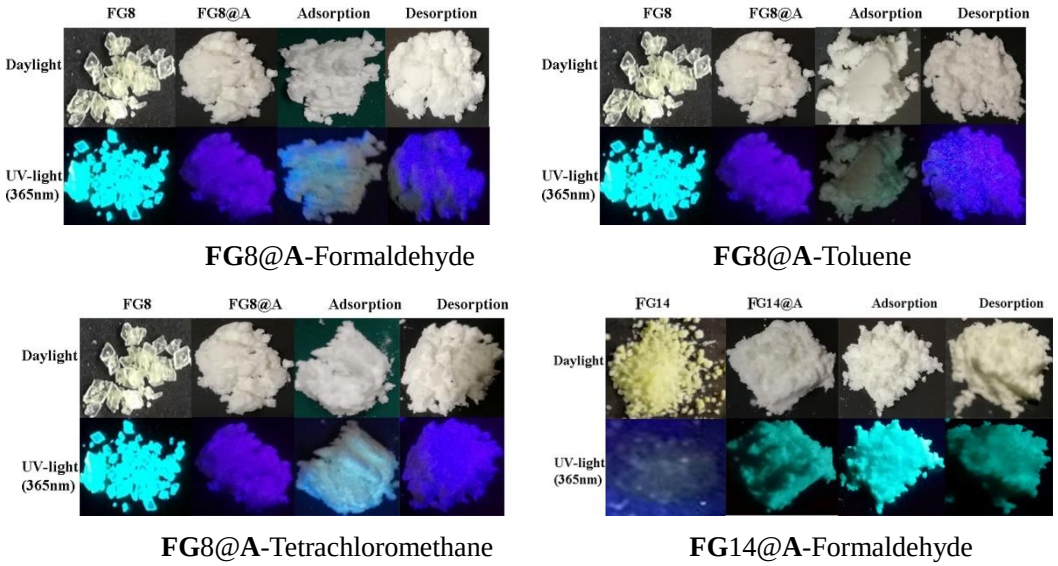

FG8@**A**-Formaldehyde **FG**8@**A**-Toluene

FG8@**A**-Tetrachloromethane **FG**14@**A**-Formaldehyde

Fig. S26. A comparison of fluorescence changes of the selected **FG**8 or 14@**A** adsorbing and desorbing the selected volatile compounds.

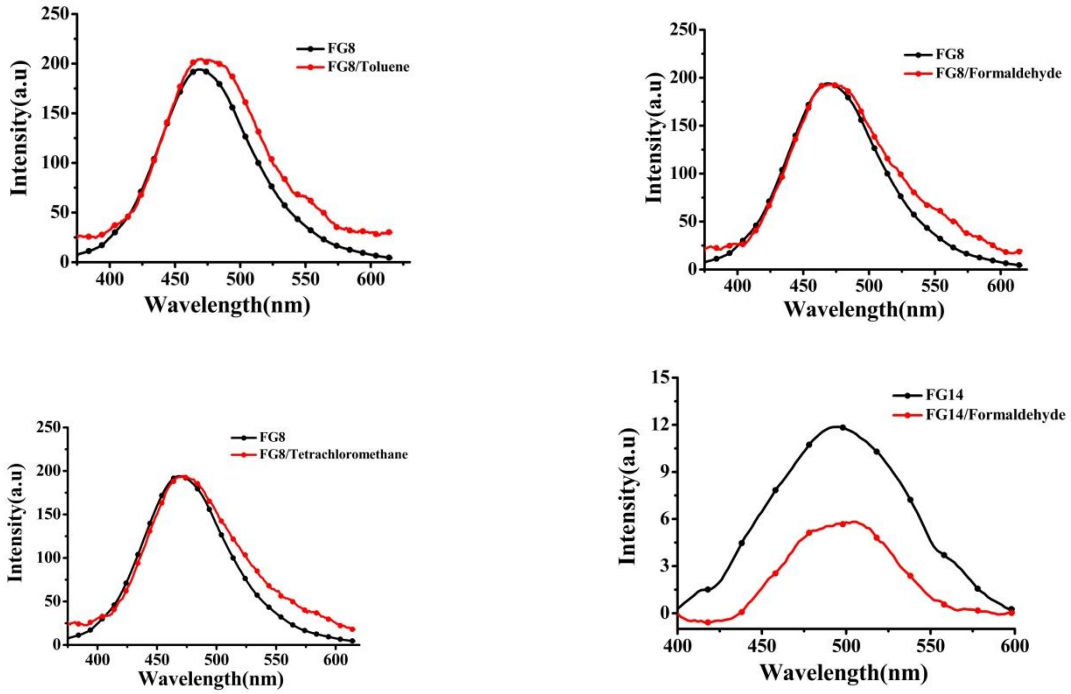

Fig. S27. Influence of the selected volatiles compounds absorbed by neat **FG**8 and **FG**14 on the fluorescence strength of the **FG**8 and **FG**14, respectively.